連遺伝子 Dysbindin1 と NRG1 の発現解析. 第 32 回日本生物学的精神医学会.福岡.10.7-9(8), 2010.ポスター

24) 椎野智子,アレクシッチ ブランコ,久島周,伊藤圭人,中村由嘉子,氏家寛,鈴木道雄,稲田俊也,橋本亮太,武田雅俊,岩田仲生,尾崎紀夫. KREMEN1 および DKK1 を候補遺伝子とした日本人統合失調症の関連研究. 第 32 回日本生物学的精神医学会.福岡.10.7-9(8), 2010.ポスター

25) 大井一高,橋本亮太,安田由華, 福本素由己,山森英長,紙野晃人,池澤浩二,疇地道代,岩瀬真生,数井裕光,笠井清登,武田雅俊. SIDMAR1 遺伝子の Gln2Pro 多型は統合失調症のリスク及び前頭前皮質の賦活化と関連する. 第 32 回日本生物学的精神医学会.福岡.10.7-9(9), 2010.ポスター

26) 太田深秀,藤井崇,根本清貴,大西隆,守口善也,橋本亮太,佐藤典子,功刀浩. 統合失調症発症リスク及び疾患に伴う大脳形態変化と ABCA1 遺伝子多型との関連解析. 第 32 回日本生物学的精神医学会.福岡.10.7-9(9), 2010.ポスター

27) 安田由華,橋本亮太,山森英長,大井一高,福本素由己,高村 明孝,毛利 育子,谷池 雅子,武田雅俊. 広汎性発達障害におけるリンパ芽球を用いた mRNA 発現定量解析についての検討. 第 32 回日本生物学的精神医学会.福岡.10.7-9(9).2010.ポスター

28) 福本素由己, 橋本亮太, 安田由華,大井一高, 山森英長,井池直美,岩瀬真生, 数井裕光,武田雅俊. 統合失調症における Remission の研究. 第32回日本生物学的精神医学会.福岡.10.7-9(9), 2010.ポスター

29) 橋本亮太、統合失調症の新しい理解に向けて、日本心理学会第 74 回大会、大阪、9.20-22(21), 2010. 招待講演

30) 橋本亮太、オーガナイザー、スタディーグループ 4「発達障害治療薬の現状と展望」、第 20 回日本臨床精神神経薬理学会・第 40 回日本神経精神薬理学会合同年会、仙台、9.14-16(15), 2010

31) Yamamori H. **Hashimoto R.** Takamura H. Verrall L. Yasuda Y. Ohi K. Fukumoto M. Ito A. Takeda M. Dysbindin1 and NRG1 genes expression in immortalized lymphocytes from patients with schizophrenia. Neuro2010、神戸、9.2-4(3), 2010

32) 橋本亮太、統合失調症の認知機能障害に対する遺伝子研究はどこまで到達したか？、シンポジウム「統合失調症の認知機能障害のメカニズム-その到達点と将来の展望」、神戸、Neuro2010、9.2-4(4), 2010. 招待講演

33) 山森英長、橋本亮太、高村明孝、Verrall Louise、安田由華、大井一高、福本素由己、伊藤彰、武田雅俊、統合失調症患者由来のリンパ芽球における、統合失調症関連遺伝子、Dysbindin1、NRG1、の発現、Neuro2010、神戸、9.2-4(3), 2010. ポスター

34) Katsunori Kobayashi, Hironori Takamura, Masatoshi Takeda, Hidenori Suzuki, Ryota Hashimoto, Correlated changes in serotonergic and dopaminergic synaptic modulations in mice lacking the schizophrenia susceptibility gene dysbindin, Neuro2010、神戸、9.2-4(3), 2010. 口演

35) Iwase M, Azechi M, Ikezawa K, Ishii R,Takahashi H, Nakahachi T, Canuet L, Y Aoki, Kurimoto R, Kazui H, Fukumoto M, Iike N, Ohi K, Yamamori H, Yasuda Y, **Hashimoto R**, Takeda M.Two-channel near infrared spectroscopy activation curves of oxyhemoglobin during frontal tasks in schizophrenia、Neuro2010、神戸、9.2-4(3), 2010. ポスター

36) 橋本亮太、統合失調症、精神医学研修コース「ここまでわかった精神疾患の脳内メカニズム」、第 106 回日本精神神経学会、広島、5.20-22(22), 2010. 招待

37) 橋本亮太、大井一高、安田由華、福本素由己、岩瀬真生、井池直美、疇地道代、池澤浩二、高屋雅彦、高橋秀俊、石井良平、数井裕光、岩田仲生、武田雅俊、統合失調症のゲノムワイド関連解析にて見出された ZNF804A 遺伝子のリスク多型は統合失調症の記憶機能と関連する、第 106 回日本精神神経学会、広島、5.20-22(22), 2010.口演

38) 安田由華、橋本亮太、山森英長、大井一高、福本素由己、武田雅俊、広汎性発達障害におけるリンパ芽球を用いた mRNA 発現定量解析についての検討、第 106 回日本精神神経学会、広島、5.20-22(21)、2010. ポスター

39) 大井一高、橋本亮太、安田由華、福本素由己、井池直美、山森英長、谷向仁、田上真次、森原剛史、大河内正康、田中稔久、工藤喬、岩瀬真生、数井裕光、武田雅俊、統合失調症における TCI によるパーソナリティー傾向: 日本人患者対照研究及びメタ解析からのエビデンス、第 106 回日本精神神経学会、広島、5.20-22(20), 2010.ポスター

G. 知的財産権の出願・登録状況（予定を含む）

1. 特許取得
該当なし。

2. 実用新案登録
該当なし。

3. その他
該当なし。

平成２２年度厚生科学研究費補助金（障害者対策総合研究事業）
分担研究報告書

超細密染色体分析から捉え直すヒト発達障害研究

分担研究課題：年齢依存性てんかん性脳症の遺伝型と臨床型の関連性の解明

分担研究者　加藤光広　山形大学医学部小児科学講座

研究要旨：
大田原症候群29例，ウエスト症候群54例に対して*STXBP1*遺伝子解析を行い，新たに病的変異を示した９例と，過去に変異を同定した５例との 14 例に対し，臨床解析を行った。てんかんのタイプは全例大田原症候群で，ウエスト症候群ではみいだされなかった。てんかん発作は難治例が多いが，TRH, ACTH, PB などが発作軽減や一時的な抑制に有効であった。てんかん以外の症状は，歩行可能は１例のみで他は全例重度の運動障害に加え重度の精神遅滞を呈していた。頭部 MRI は，乳児期のごく早期には全例正常であったが，その後には軽度の脳萎縮を示す例が多かった。歩行可能例は発作抑制が長期得られており，脳萎縮もなく，遺伝子異常であっても機能予後の改善のためには発作の抑制が重要と考えられる。

A．研究目的

年齢依存性てんかん性脳症は，てんかんに加え認知機能や運動障害などの発達障害を併発する疾患であり，発達期に応じた特徴的な発作型や脳波所見によって分類される複数のてんかん症候群で構成されている。新生児期に発症する大田原症候群と乳児期に発症するウエスト症候群は，年齢依存性てんかん性脳症の代表的疾患である。私たちは2008年に*STXBP1*が大田原症候群の原因遺伝子であることを明らかにしたが，その後の欧州からの報告では，*STXBP1* 変異は非特異的な乳幼児期発症のてんかん性脳症やウエスト症候群で同定され，大田原症候群では同定されないなど，*STXBP1* 変異の臨床像がまだ十分明らかになっていない。

本研究では，*STXBP1* 遺伝子変異による臨床型を明らかにする事を目的とした。

B．研究方法

①保護者の承諾を得て，脳形成異常や代謝異常，周産期障害による明らかな原因を除外された年齢依存性てんかん性脳症の患者（大田原症候群29例，ウエスト症候群 54 例）および両親の血液から DNA を抽出し，さらに臨床情報（発作型・脳波・頭部 MRI・使用薬剤と効果・併発症など）を収集した。

②*STXBP1* 遺伝子の全コード領域を high resolution melting (HRM)法を用いて変異スクリーニングを行い，陽性例に対して直接塩基配列の解析を行った。なお，男性では*ARX*遺伝子を，女性では*CDKL5*遺伝子の変異スクリーニングを行い，それぞれの変異例は除外した。

③今回新規に *STXBP1* 変異を同定した症例と，過去に変異を同定した *STXBP1* 変異例の臨床情報をまとめ，大田原症候群の既報告例と比較した。

C．研究結果

①②大田原症候群 9 例において *STXBP1* 変異を同定した。内訳はナンセンス変異 3 例，フレームシフト変異 2 例，スプライシング異常 1 例，ミスセンス変異 3 例で，全例新生変異であった。ミスセンス変異は 3 例とも c.1217G>A (p.R406H)変異であったが，その他の変異部位は散在していた。ウエスト症候群では変異が同定されなかった。

①③*STXBP1* 変異例合計 14 例は全例大田原症候群であり，そのうち 11 例(79%)は，大田原症候群からウエスト症候群に移行した。大田原症候群の発症時期は平均 1.4 か月であり，ウエスト症候群への移行時期は平均4.7か月であった。5例(ACTH 2 例，TRH2 例，ビタミン B6 とニトラゼパム併用 1 例)は治療に反応し発作が消失したが，4 例はその後再発し，発作の長期緩解例は 1 例のみであった。発作に対し部分的に有効だった薬剤はフェノバール(PB)，ゾニサミド(ZNS)，バルプロ酸(VPA)，ベンゾジアゼピン系であったが，無効例も多く，ACTH のみが有効 7 例，無効 0 例と差を認めた。

全例で精神遅滞の併発を認め，生後6か月の中等度例を除き，13例は最重度であった。運動機能は12例が未獲定，1例が寝返りレベルで，歩行可能例は乳児期に発作が消失した非再発・長期緩解の1例であった。乳児早期（0〜3か月）にMRIが撮影された7例は全例正常であったが，その後3か月から3歳時点のMRIでは9例中6例に軽度の脳萎縮を認めた。

D．考察

今回新たに29例中9例の大田原症候群で*STXBP1*に変異を認め，合計43例中14例，33%の変異率であった。*STXBP1*は，脳形成障害等を除いた原因不明の大田原症候群における主要な原因であることが確認された。最初の報告では微細欠失例を除きミスセンス変異のみであったが，今回9例中6例はナンセンス変異やフレームシフト変異，スプライシング異常であり，*STXBP1*のハプロ不全が原因と考えられた。

既報告と比べ，ウエスト症候群への移行率に明らかな差はなかったが，大田原症候群の発症時期は既報告では75%は新生児期(1か月未満)であり，*STXBP1*変異例では発症が遅かった。既報告では脳形成障害の報告が多いが，*STXBP1*変異例では発症時のMRIは正常であり，既報告例に比べ形態的には軽症であることが影響している可能性がある。しかし，*STXBP1*変異例でも発作は難治で，認知機能，運動機能ともに重症例が多く，経過とともに脳萎縮が出現する。運動予後が良かった1例は，発作も抑制されており，脳萎縮はなく，機能予後改善のためには発作コントロールが重要である。ACTH以外に有効性に差のある治療薬剤は明らかにできなかったが，近年国内でも保険適応となったガバペンチン，トピラマート，ラモトリギン，レベチラセタムなどの新規抗てんかん薬の使用例は少なく，今後検討が必要である。

E．結論

*STXBP1*のハプロ不全は大田原症候群の主要な原因遺伝子であり，既報告と比べ発症が遅い。機能予後改善のためには，遺伝子異常の場合でも，発作の抑制が重要と考えられる。

F．健康危険情報

特になし。

G．研究発表

1．論文発表

Saitsu H, Hoshino H, Kato M, Nishiyama K, Okada I, Yoneda Y, Tsurusaki Y, Doi H, Miyake N, Kubota M, Hayasaka K, Matsumoto N. Paternal mosaicism of an *STXBP1* mutation in OS. *Clin Genet*, in press

Kato M, Koyama N, Ohta M, Miura K, Hayasaka K. Frameshift mutations of the *ARX* gene in familial Ohtahara syndrome. *Epilepsia* 51:1679-1684, 2010

Saitsu H, Tohyama J, Kumada T, Egawa K, Hamada K, Okada I, Mizuguchi T, Osaka H, Miyata R, Furukawa T, Haginoya K, Hoshino H, Goto T, Hachiya Y, Yamagata T, Saitoh S, Nagai T, Nishiyama K, Nishimura A, Miyake N, Komada M, Hayashi K, Hirai S, Ogata K, Kato M, Fukuda A, Matsumoto N. Dominant-negative mutations in alpha-II spectrin cause West syndrome with severe cerebral hypomyelination, spastic quadriplegia, and developmental delay. *Am J Hum Genet* 86:881-891, 2010

Shiihara T, Maruyama K, Yamada Y, Nishimura A, Matsumoto N, Kato M, Sakazume S. A case of Baraitser-Winter syndrome with unusual brain MRI findings: pachygyria, subcortical-band heterotopia, and periventricular heterotopia. *Brain Dev* 32:502-505, 2010

Kanazawa K, Kumada S, Kato M, Saitsu H, Kurihara E, Matsumoto N. Choreo-ballistic movements in a case carrying a missense mutation in syntaxin binding protein 1 gene. *Mov Disord* 25:2265-2267, 2010

加藤光広. 脳形成障害・てんかんのトピックス— 年齢依存性てんかん性脳症と介在ニューロン病—. 脳と発達 42:333-338, 2010

学会発表

Mitsuhiro Kato, Hirotomo Saitsu,Ippei Okada,Kenji E. Orii,Tsukasa Higuchi, Hideki Hoshino, Masaya Kubota, Hiroshi Arai, Tetsuzo Tagawa, Shigeru Kimura, Akira Sudo, Sahoko Miyama, Yuichi Takami, Toshihide Watanabe, Akira Nishimura, Kiyomi Nishiyama, Noriko Miyake, Takahito Wada, Hitoshi Osaka, Naomi Kondo, Kiyoshi Hayasaka, Naomichi Matsumoto: Haploinsufficiency of *STXBP1* is an important cause for Ohtahara syndrome, but not for cryptogenic West syndrome. 8th Asian & Oceanian Epilepsy Congress, Melbourne Convention and Exhibition Centre, Melbourne, Australia, October 21-24, 2010

Jun Tohyama, Hirotomo Saitsu, Noriyuki Akasaka, Hitoshi Osaka, Rie Miyata, Mitsuhiro Kato, Naomichi Matsumoto: A new clinical epileptic syndrome caused by *SPTAN1* mutation. 8th Asian & Oceanian Epilepsy Congress, Melbourne Convention and Exhibition Centre, Melbourne, Australia, October 21-24, 2010

H．知的財産権の出願・登録状況

なし

平成２２年度厚生科学研究費補助金（障害者対策総合研究事業）
分担研究報告書

超細密染色体分析から捉え直すヒト発達障害研究

分担研究課題： クレアチン欠損症の簡便なスクリーニング法の開発

分担研究者　　小坂仁 神奈川県立こども医療センター神経内科、

研究要旨：
クレアチン欠損症はL-arginine: glycine amidinotransferase欠損症, guanidinoacetate methyltransferase欠損症, creatine transporter欠損症.よりなり、共通の症状として精神遅滞、自閉症、てんかんを持つ。精神遅滞の2%前後を占めるとも言われるが、本邦での報告例はなく、その頻度も不明である。クレアチン欠損症の診断法としては、質量分析計を用いた測定法が一般的であり、一般的な普及となっていない。我々は、HPLCを用いた簡便なスクリーニング法を開発した。この方法を用い、本邦初症例を見出した。

A．研究目的

クレアチン欠損症（Cerebral creatine deficiency syndromes : CCDS ） は L-arginine: glycine amidinotransferase (AGAT)欠損症, guanidinoacetate methyltransferase (GAMT) 欠損症, creatine transporter (SLC6A8) 欠損症.よりなり、共通の症状として精神遅滞、自閉症、てんかんを持つ。いくつかの報告では精神遅滞の 2%前後を占めると言われ、AGAT欠損症は5例, GAMT欠損症は37例、SLC6A8欠損症は150例以上の報告がある。いずれも本邦での報告例はなく、その頻度も不明である。また診断としては、高速クロマトグラフィーと質量分析を組み合わせた方法が主として用いられているが、利用出来る施設は限られており、より簡便なスクリーニング方法が求められている。今回の目的は、CCDSのより簡便なスクリーニング方法の開発を目的とした。

B．研究方法

CCDSの3疾患は3つの化合物、CR:クレアチン、GAA：グアニジノ酢酸、GN：クレアチニンを測定することでスクリーニング可能である。 すなわちAGAT欠損症; GAA/CN↓CR/CN↓、GAMT欠損症;GAA/CN↑CR/CN↓、SLC6A8欠損症;GAA/CN正常、CR/CN↑のプロフィールをもつ。今回我々は、高速液体クロマトグラフィー (HPLC)を用いカラム、溶出条件を検討することにより、これらの化合物を迅速に同定する条件検討を行った。またこの方法で当院の原因不明の発達遅滞の患者のスクリーニングを行った、凍結尿500 μlを等量のアセトニトリル添加後、遠心分離し、25 μlを解析に用いた

C．研究結果

①弱酸性陽イオン交換カラムを用い、リン酸バッファーの濃度を変えることにより、UV で CR：(5.54±0.0035) min、 GAA： (6.41±0.0079) min、GN： (13.53±0.046)min で検出する条件を見出した。これらは再現性よく短時間で検出可能であり、誘導化が必要なく、一般的なバッファーを用いており、高価な質量分析計を必要としないため、今後多くの施設で用いられる可能性がある。
②この系を用いて、当院の精神遅滞症例 89 名のスクリーニングを行い、3名でCR/CN↑を認めた。そのうち1例では磁気共鳴分光法で大脳におけるCR ピークの消失が消失しており、線維芽細胞を用いた取り込み試験でも、正常にくらべCRの細胞内への取り込みの有意な低下を認めた。以上よりSLC6A8欠損症を強く疑い、SLC6A8遺伝子解析を行ったところ遺伝子の全欠失を確認し、切断点の塩基配列も同定した。

D．考察

簡便なスクリーニング法の開発により、本邦におけるCCDSの頻度が明らかになる可能性がある。

E．結論

今回我々は、簡便なCCDSスクリーニング法を開発し、本邦初症例を見出した。

G．研究発表

1．論文発表

1. Osaka H, Koizume S, Aoyama H, Iwamoto H, Kimura S, Nagai , Kurosawa K, Yamashita S. Mild phenotype in Pelizaeus-Merzbacher disease caused by a PLP1-specific mutation, *Brain Dev.* 2010 32; 703-707

2. Osaka H, Hamanoue H, Yamamoto R, Nezu A, Sasaki M, Saitsu H, Kurosawa K, Shimbo H, Matsumoto N, Inoue K. Disrupted SOX10 regulation of GJC2 transcription causes Pelizaeus-Merzbacher-Like Disease . *Ann Neurol*, 2010; 68: 250-4.

3. Saitsu H, Kato M, Okada I, Orii KE, Higuchi T, Hoshino H, Kubota M, Arai H,Tagawa T, Kimura S, Sudo A, Miyama S, Takami Y, Watanabe T, Nishimura A,Nishiyama K, Miyake N, Wada T, Osaka H, Kondo N, Hayasaka K, Matsumoto N. STXBP1 mutations in early infantile epileptic encephalopathy with suppression-burstpattern. *Epilepsia,* 51:2397–2405, 2010

Tsuji M, Aida N, Obata T, Tomiyasu M, Furuya N, Kurosawa K, Errami A, Gibson KM, Salomons GS, Jakobs C, Osaka H. A new case of GABA transaminase deficiency facilitated by proton MR spectroscopy. *J Inherit Metab Dis*. 2010:33; 85-90.

5. Tsuyusaki Y, Yoshihashi H, Furuya N, Adachi M, Osaka H, Yamamoto K, Kurosawa K. 1p36 deletion syndrome associated with Prader-Willi-like phenotype. *Pediatr Int.* 2010; 52: 547-550

6. Sato I, Onuma A, Goto N, Sakai F, Fujiwara I, Uematsu M, Osaka H, Okahashi S, Nonaka I, Tanaka S, Haginoya K. A case with central and peripheral hypomyelination with hypogonadotropic hypogonadism and hypodontia (4H syndrome) plus cataract. *J Neurol Sci.* 2011; 300;179-181

7. Tsuji M, Takagi A, Sameshima K, Iai M, Yamashita S, Shinbo H, Furuya N, Kurosawa K, Osaka H. 5,10-Methylenetetrahydrofolate reductase deficiency withprogressive polyneuropathy in an infant. *Brain Dev.* 2010 [Epub]

8. Natsuga K, Nishie W, Shinkuma S, Arita K, Nakamura H, Ohyama M, Osaka H, Kambara T, Hirako Y, Shimizu H. Plectin deficiency leads to both muscular dystrophy and pyloric atresia in epidermolysis bullosa simplex. *Hum Mutat.* 2010: 31; E1687-98.

9. Muto A, Oguni H, Takahashi Y, Shirasaka Y, Sawaishi Y, Yano T, Hoshida T, Osaka H, Nakasu S, Akasaka N, Sugai K, Miyamoto A, Takahashi S, Suzuki M, Ohmori I,Nabatame S, Osawa M. Nationwide survey (incidence, clinical course, prognosis) of Rasmussen's Encephalitis. *Brain Dev.* 2010;32:445-53

10. Saitsu H, Tohyama J, Kumada T, Egawa K, Hamada K, Okada I, Mizuguchi T, Osaka H, Miyata R, Furukawa T, Haginoya K, Hoshino H, Goto T, Hachiya Y, Yamagata T,Saitoh S, Nagai T, Nishiyama K, Nishimura A, Miyake N, Komada M, Hayashi K, HiraiS, Ogata K, Kato M, Fukuda A, Matsumoto N. Dominant-negative mutations inalpha-II spectrin cause West syndrome with severe cerebral hypomyelination,spastic quadriplegia, and developmental delay. *Am J Hum Genet.* 2010;86:881-91.

B．学会発表

1. 辻 恵、三谷忠宏、渡辺好宏、鮫島希代子、和田敬仁、井合瑞江、山下純正、小坂仁、急性脳症を呈した重症乳児ミオクロニーてんかんの 1 例、第 65 回神奈川てんかん懇話会 2010.1.16 横浜

2. 大脳白質変性を伴う交通性水頭症に末梢神経障害・呼吸不全を合併した乳児例辻 恵、渡辺好宏、鮫島希代子、和田敬仁、井合瑞江、山下純正、小坂 仁, 第 15 回蔵王セミナー 2010.2.20-21 山形

3. インフルエンザ罹患に伴うせん妄の Delirium Rating Scale による検討
渡辺好宏、藤田利治、和田敬仁、小坂仁、森雅亮、横田俊平第 113 回日本小児科学会総会 2010.4.24 盛岡

4. MRS が診断に有用であった Creatine

transporter deficiency（CTD）の一例 露崎悠、高木篤史、渡辺好宏、辻恵、鮫島希代子、和田敬仁、井合瑞江、山下純正、新家敏弘、久原とみ子、相田典子、小坂仁、 第 52 回関東小児神経学会 22.3.20 東京

5. 抗NMDA 受容体脳炎の 1 例, 秋庭真理子、渡辺好宏、辻恵、和田敬仁、井合瑞江、山下純正、小坂仁, 山岡正慶、的場香織、第 46 回神奈川小児神経学会、2010.7.10 横浜

6. 小児期発症 Charcot-Marie-Tooth 病の臨床病理学的および遺伝学的検討山下純正、渡辺好、辻恵、鮫島希代子、和田敬仁、井合瑞江、小坂仁, 阿部暁子、早坂清、 第 52 回日本小児神経学会 5 月 20 日～22 日福岡

7. 精神遅滞患者に対するクレアチニン代謝異常のスクリーニング法の開発、和田敬仁、新保裕子、小坂仁、第 52 回日本小児神経学会 5 月 20 日福岡

8. 大脳白質変性を伴う交通性水頭症に末梢神経障害・呼吸不全を合併した MTHFR 欠損症の一例, 辻 恵、渡辺好宏、鮫島希代子、和田敬仁、井合瑞江、山下純正、小坂 仁、第 52 回日本小児神経学会 5 月 20 日福岡

9. 新型インフルエンザによる急性脳症の臨床的検討, 渡辺好宏、安西里恵、露崎悠、辻恵、鮫島希代子、和田敬仁、井合瑞江、小坂仁、山下純正, 第 52 回日本小児神経学会 5 月 20 日福岡

10. サイクロフォスファマイド療法が著効した抗 NMDA 受容体抗体脳炎の 1 例、三谷忠宏、大塚佳満、和田敬仁、辻恵、渡辺好宏、井合瑞江、山下純正、小坂仁、第 53 回関東小児神経学会 22.9.11 東京

G．知的所有権の取得状況

特願 2010-25346 弱酸性陽イオン交換カラムを用いた生体アミンの検出。

研究成果の刊行に関する一覧表

書籍

著者氏名	論文タイトル名	書籍全体の編集者名	書　籍　名	出版社名	出版地	出版年	ページ

雑誌

発表者氏名	論文タイトル名	発表誌名	巻号	ページ	出版年
Shiihara T, others, Matsumoto N, others.	A case of Baraitser-Winter syndrome with unusual brain MRI findings of pachygyria, subcortical band heterotopia and periventricular heterotopias.	Brain Dev	32(6)	502-505	2010
Saitsu H, others, Matsumoto N	Dominant negative mutations in α-II spectrin cause early onset West syndrome with severe cerebral hypomyelination, spastic quadriplegia, and developmental delay.	Am J Hum Genet	86(6)	881-889	2010
Saitsu H, others, Matsumoto N	*STXBP1* mutations in severe infantile epilepsies with suppression-burst pattern.	Epilepsia	51(12)	2397-2405	2010
Sakai H, others, Matsumoto N	Analysis of an insertion mutation in a cohort of 93 patients with spinocerebellar ataxia type 31 (SCA31) from Nagano, Japan.	Neurogenet	11(4)	409-415	2010
Osaka H, others, Matsumoto N, Inoue K.	Disrupted SOX10 regulation of GJC2 transcription causes Pelizaeus-Merzbacher-Like Disease.	Ann Neurol	68(2)	250-254	2010
Nishimura A, others, Matsumoto N	*De novo* deletion of 1q24.3-q31.2 in a patient with severe growth retardation.	Am J Med Genet	152A(5)	1322-1325	2010
Komoike Y, others, Matsumoto N, others.	Zebrafish gene knockdowns imply roles for human *YWHAG* in infantile spasms and cardiomegaly.	Genesis	48(4)	233-243	2010

発表者氏名	論文タイトル名	発表誌名	巻号	ページ	出版年
Doi H, others, Matsumoto N, others.	Siblings with the adult-onset slowly progressive type of pantothenate kinase-associated neurodegeneration and a novel mutation, Ile346Ser, in PANK2: Clinical features and (99m)Tc-ECD brain perfusion SPECT findings.	J Neurol Sci	290 (1-2)	172-176	2010
Miyake N, others, Matsumoto N.	Loss of decorin dermatan sulfate impairing collagen bundle formation in a new type of Ehlers-Danlos syndrome.	Hum Mut	31(8)	966-974	2010
Kosho T, others, Matsumoto N.	A New Ehlers-Danlos Syndrome With Craniofacial Characteristics, Multiple Congenital Contractures, Progressive Joint and Skin Laxity, and Multisystem Fragility-related Manifestations.	Am J Med Genet	152A (6)	1333-1346	2010
Kimura S, others, Matsumoto N, Ishibashi M.	Rudimentary Claws and Pigmented Nail-like Structures on the Distal Tips of the Digits of *Wnt7a* Mutant Mice: *Wnt7a* Suppresses Nail-like Structure Development in Mice.	Birth Defects Res A Clin Mol Teratol	88(6)	487-496	2010
Kanazawa K, others, Matsumoto N	Choreo-ballistic movements in a case carrying a missense mutation in syntaxin binding protein 1 gene.	Mov Disord	25(13)	2265-2267	2010
Ng S, others, Matsumoto N, others.	Exome sequencing identifies *MLL2* mutations as a cause of Kabuki syndrome.	Nat Genet	42(9)	790-793	2010
Yamada-Okabe T, others, Matsumoto N.	Functional characterization of the zebrafish *WHSC1*-related gene, a homologue of human *NSD2*.	Biochem Biophys Res Commun	402(2)	335-339	2010
Okada I, others, Matsumoto M, Saitsu H.	*SMOC1* is essential for ocular and limb development in humans and mice.	Am J Hum Genet	88(1)	30-41	2011
Tohyama J, others, Matsumoto N.	Dandy-Walker malformation associated with heterozygous *ZIC1* and *ZIC4* deletion: Report of a new patient.	Am J Med Genet	155A(1)	130-131	2011
Furuichi T, others, Matsumoto N, others.	*CANT1* is also responsible for Desbuquois dysplasia, type 2 and Kim variant.	J Med Genet	48(1)	32-37	2011

発表者氏名	論文タイトル名	発表誌名	巻号	ページ	出版年
Kato M, et al.	Frameshift mutations of the *ARX* gene in familial Ohtahara syndrome.	*Epilepsia*	51	1679-1684	2010
Shiihara T, et al., Kato M	Peripheral lymphocyte subset and serum cytokine profiles of patients with West syndrome.	*Brain Dev*	32	695-702	2010
Hosokawa S, et al., Okamoto N	A case of Brachmann-de Lange syndrome with congenital diaphragmatic hernia and *NIPBL* gene mutation	Congenit Anom (Kyoto).	50	129-132	2010
Kobayashi T, et al., Okamoto N, et al.	Molecular and clinical analysis of RAF1 in Noonan syndrome and related disorders: dephosphorylation of serine 259 as the essential mechanism for mutant activation.	Hum Mutat.	31	284-294	2010
Okamoto N, et al.	Co-occurrence of Prader-Willi and Sotos syndromes.	Am J Med Genet A.	152A	2103-2109	2010
Komatsuzaki S, et al., Okamoto N, et al.	Mutation analysis of the SHOC2 gene in Noonan-like syndrome and in hematologic malignancies.	J Hum Genet	55	801-809	2010
Takanashi J, et al., Okamoto N, et al.	Neuroradiologic features of CASK mutations.	Am J Neuroradiol.	31	1619-1622	2010
Hayashi S, et al., Okamoto N, et al.	Clinical application of array-based comparative genomic hybridization by two-stage screening for 536 patients with mental retardation and multiple congenital	J Hum Genet	印刷中		2011
Filges I, et al., Okamoto N, et al.	Reduced expression by SETBP1 haploinsufficiency causes developmental and expressive language delay indicating a phenotype distinct from Schinzel-Giedion syndrome.	J Med Genet	印刷中		2011
Hashimoto R, et al.	The Impact of a Genome-Wide Supported Psychosis Variant in the ZNF804A Gene on Memory Function in Schizophrenia.	Am J Med Genet B Neuropsychiatr Genet,	153B(8)	1459-64	2010
Yasuda Y, Hashimoto R, et al.	Association study of *KIBRA* gene with memory performance in a Japanese population.	The World Journal of Biological Psychiatry,	11(7)	852-7	2010
Osaka H, et al.	Mild phenotype in Pelizaeus-Merzbacher disease caused by a PLP1-specific mutation,	Brain Dev.	32	703-707	2010

発表者氏名	論文タイトル名	発表誌名	巻号	ページ	出版年
Tsuji M, et al., Osaka H.	A new case of GABA transaminase deficiency facilitated by proton MR spectroscopy.	J Inherit Metab Dis.	85-90	33	2010
Tsuyusaki Y, et al., Osaka H, et al.	1p36 deletion syndrome associated with Prader-Willi-like phenotype.	Pediatr Int	547-555	52	2010
Sato I, et al., Osaka H, et al.	A case with central and peripheral hypomyelination with hypogonadotropic hypogonadism and hypodontia (4H syndrome) pl	J Neurol Sci.	300	179-181	2011;
Natsuga K, et al., Osaka H, et al.	Plectin deficiency leads to both muscular dystrophy and pyloric atresia in epidermolysis bullosa simplex.	*Hum Mutat*	31	E1687-1698.	2010
Muto A, et al., Osaka H, et al.	Nationwide survey (incidence, clinical course, prognosis) of Rasmussen's Encephalitis.	Brain Dev	32	445-453	2010
小坂 仁	脊髄小脳変性症	小児の治療指針（診断と治療社）	増刊号	760-762	2010

Dominant-Negative Mutations in α-II Spectrin Cause West Syndrome with Severe Cerebral Hypomyelination, Spastic Quadriplegia, and Developmental Delay

Hirotomo Saitsu,[1,*] Jun Tohyama,[2] Tatsuro Kumada,[3] Kiyoshi Egawa,[3] Keisuke Hamada,[4] Ippei Okada,[1] Takeshi Mizuguchi,[1,17] Hitoshi Osaka,[5] Rie Miyata,[6] Tomonori Furukawa,[3] Kazuhiro Haginoya,[7] Hideki Hoshino,[8] Tomohide Goto,[9] Yasuo Hachiya,[10] Takanori Yamagata,[11] Shinji Saitoh,[12] Toshiro Nagai,[13] Kiyomi Nishiyama,[1] Akira Nishimura,[1] Noriko Miyake,[1] Masayuki Komada,[14] Kenji Hayashi,[15] Syu-ichi Hirai,[15] Kazuhiro Ogata,[4] Mitsuhiro Kato,[16] Atsuo Fukuda,[3] and Naomichi Matsumoto[1,*]

A de novo 9q33.3-q34.11 microdeletion involving *STXBP1* has been found in one of four individuals (group A) with early-onset West syndrome, severe hypomyelination, poor visual attention, and developmental delay. Although haploinsufficiency of *STXBP1* was involved in early infantile epileptic encephalopathy in a previous different cohort study (group B), no mutations of *STXBP1* were found in two of the remaining three subjects of group A (one was unavailable). We assumed that another gene within the deletion might contribute to the phenotype of group A. *SPTAN1* encoding α-II spectrin, which is essential for proper myelination in zebrafish, turned out to be deleted. In two subjects, an in-frame 3 bp deletion and a 6 bp duplication in *SPTAN1* were found at the initial nucleation site of the α/β spectrin heterodimer. *SPTAN1* was further screened in six unrelated individuals with WS and hypomyelination, but no mutations were found. Recombinant mutant (mut) and wild-type (WT) α-II spectrin could assemble heterodimers with β-II spectrin, but α-II (mut)/β-II spectrin heterodimers were thermolabile compared with the α-II (WT)/β-II heterodimers. Transient expression in mouse cortical neurons revealed aggregation of α-II (mut)/β-II and α-II (mut)/β-III spectrin heterodimers, which was also observed in lymphoblastoid cells from two subjects with in-frame mutations. Clustering of ankyrinG and voltage-gated sodium channels at axon initial segment (AIS) was disturbed in relation to the aggregates, together with an elevated action potential threshold. These findings suggest that pathological aggregation of α/β spectrin heterodimers and abnormal AIS integrity resulting from *SPTAN1* mutations were involved in pathogenesis of infantile epilepsy.

Introduction

West syndrome (WS) is a common infantile epileptic syndrome characterized by brief tonic spasms, an electroencephalogram pattern called hypsarrhythmia, and mental retardation.[1] Brain malformations and metabolic disorders can be underlying causes of WS, but many cases remain etiologically unexplained.[1] Only two causative genes, *ARX* (MIM *300382) and *CDKL5* (MIM *300203), are mutated in a subset of familial and sporadic X-linked WS cases (ISSX1 and ISSX2 [MIM #308350 and #300672]).[2–4] Early infantile epileptic encephalopathy with suppression-burst (EIEE) is the earliest form of infantile epileptic syndrome.[5,6] The transition from EIEE to WS occurs in 75% of individuals with EIEE, suggesting a common pathological mechanism between these two syndromes.[5,6] We have recently reported that de novo mutations of *STXBP1* (MIM *602926) cause EIEE.[7]

Spectrins are submembranous scaffolding proteins involved in the stabilization of membrane proteins.[8,9] Spectrins are flexible and long molecules consisting of α and β subunits, which are assembled in an antiparallel side-by-side manner into heterodimers. Heterodimers form by end-to-end tetramers integrating into the membrane cytoskelton.[8,9] The spectrin repertoire in humans includes two α subunits and five β subunits. Defects of erythroid α-I and β-I spectrins and neuronal β-III spectrin are associated with hereditary spherocytosis (SPH3 and SPH2 [MIM

[1]Department of Human Genetics, Yokohama City University Graduate School of Medicine, 3-9 Fukuura, Kanazawa-ku, Yokohama 236-0004, Japan; [2]Department of Pediatrics, Epilepsy Center, Nishi-Niigata Chuo National Hospital, 1-14-1 Masago, Nishi-ku, Niigata 950-2085, Japan; [3]Department of Physiology, Hamamatsu University School of Medicine, 1-20-1 Handayama, Hamamatsu 431-3192, Japan; [4]Department of Biochemistry, Yokohama City University Graduate School of Medicine, 3-9 Fukuura, Kanazawa-ku, Yokohama 236-0004, Japan; [5]Division of Neurology, Clinical Research Institute, Kanagawa Children's Medical Center, 2-138-4 Mutsukawa, Minami-ku, Yokohama 232-8555, Japan; [6]Department of Pediatrics, Tokyo Kita Shakai Hoken Hospital, 4-17-56 Akabanedai, Kita-ku, Tokyo 115-0053, Japan; [7]Department of Pediatrics, Tohoku University School of Medicine, 1-1 Seiryo-machi, Aoba-ku, Sendai 980-8574, Japan; [8]Division of Neurology, National Center for Child Health and Development, 2-10-1 Okura, Setagaya-ku, Tokyo 157-8535, Japan; [9]Department of Neurology, Tokyo Metropolitan Children's Medical Center, 2-8-29 Musashidai, Fuchu 183-8561, Japan; [10]Department of Neuropediatrics, Tokyo Metropolitan Neurological Hospital, 2-6-1 Musashidai, Fuchu 183-0042, Japan; [11]Department of Pediatrics, Jichi Medical University, 3311-1 Yakushiji, Shimotsuke, Tochigi 329-0498, Japan; [12]Department of Pediatrics, Hokkaido University Graduate School of Medicine, North 15, West 7, Kita-ku, Sapporo 060-8638, Japan; [13]Department of Pediatrics, Dokkyo Medical University, Koshigaya Hospital, 2-1-50 Minami-Koshigaya, Koshigaya, Saitama 343-8555, Japan; [14]Department of Biological Sciences, Faculty of Bioscience and Biotechnology, Tokyo Institute of Technology, 4259-B-16 Nagatsuta, Midori-ku, Yokohama 226-8501, Japan; [15]Department of Molecular Biology, Yokohama City University Graduate School of Medicine, 3-9 Fukuura, Kanazawa-ku, Yokohama 236-0004, Japan; [16]Department of Pediatrics, Yamagata University School of Medicine, 2-2-2 Iida-nishi, Yamagata 990-9585, Japan
[17]Present address: Laboratory of Biochemistry and Molecular Biology, National Cancer Institute, National Institutes of Health, Building 37, Room 6050, Bethesda, MD 20892, USA
*Correspondence: hsaitsu@yokohama-cu.ac.jp (H.S.), naomat@yokohama-cu.ac.jp (N.M.)
DOI 10.1016/j.ajhg.2010.04.013.

#270970 and +182870]) and spinocerebellar ataxia type 5 (SCA5 [MIM #600224]), respectively.[8,10,11] The α-II spectrin is considered as the major α spectrin expressed in nonerythroid cells, and α-II/β-II spectrin heterodimers are the predominant species in these cells.[9,12] Abnormal development of nodes of Ranvier and destabilizing initial clusters of voltage-gated sodium channels (VGSC) were observed in zebrafish α-II spectrin mutants harboring a nonsense mutation. The mutants also showed impaired myelination in motor nerves and in the dorsal spinal cord, suggesting that α-II spectrin plays important roles in the maintenance of the integrity of myelinated axons.[13]

Here, we describe three cases of early-onset WS with cerebral hypomyelination harboring *SPTAN1* (MIM *182810) aberrations. Two individuals with in-frame mutations showed more severe phenotypes than one individual with *SPTAN1* and *STXBP1* deletion. In-frame mutations of *SPTAN1* result in aggregation of α-II (mut)/β-II and α-II (mut)/β-III spectrin heterodimers, suggesting dominant-negative effects of the mutations. Spectrin aggregation is associated with disturbed clustering of VGSC and an elevated action potential threshold. Our findings revealed essential roles of α-II spectrin in human brain development and suggest that abnormal AIS is possibly involved in pathogenesis of infantile epilepsy.

Subjects and Methods

Subjects

Subjects 1, 2, and 3 have been originally reported as three of four individuals with early onset WS, severe hypomyelination, reduced white matter, and developmental delay (group A: subjects 1, 2, and 3 were previously named as No. 2, No. 1, and No. 3, respectively, and No. 4 was unavailable for this study).[14] Subject 1 has been shown to possess a 9q33.3-q34.11 microdeletion including *STXBP1*.[7] Clinical information of these three subjects with *SPTAN1* aberrations is updated in Table S1 available online. We screened for *SPTAN1* mutations in a total of eight unrelated individuals with WS accompanied by severe hypomyelination without episodes of prenatal incidents or neonatal asphyxia (six males and two females, including subjects 2 and 3 of group A). Individuals with these two distinctive features (WS and severe hypomyelination) are relatively rare. These eight patients were totally different from the previously investigated 13 EIEE patients (group B).[7] Screening tests for metabolic disorders (lactate, amino acids, and uric organic acids) were normal in all subjects. *ARX* and *CDKL5* were not mutated in the six male and two female patients, respectively. The diagnosis was made on the basis of clinical features, including tonic spasms with clustering, arrest of psychomotor development, and hypsarrhythmia on electroencephalogram, as well as brain magnetic resonance imaging (MRI) findings. Experimental protocols were approved by the Committee for Ethical Issues at Yokohama City University School of Medicine. Informed consent was obtained from all individuals included in this study, in agreement with the requirements of Japanese regulations.

Mutation Analysis

Genomic DNA was obtained from peripheral blood leukocytes by standard methods, amplified by GenomiPhi version 2 (GE Healthcare, Buckinghamshire, UK), and used for mutational screening. Exons 2 to 57, covering the *SPTAN1* coding region (of transcript variant 1, GenBank accession number NM_001130438), were screened by high-resolution melting curve (HRM) analysis as previously described.[7] In transcript variant 2 (GenBank accession number NM_003127), the only difference is that exon 37 of variant 1 was missing. PCR conditions and primer sequences are shown in Table S2. If a sample showed an aberrant melting curve shift, the PCR product was sequenced. All mutations were also verified on PCR products directly via genomic DNA (not amplified by GenomiPhi) as a template. DNAs from 250 Japanese normal controls were screened for the two in-frame *SPTAN1* mutations by HRM analysis. Normal controls which showed aberrant melting curve shift were sequenced.

Parentage Testing

For all families showing de novo mutations, parentage was confirmed by microsatellite analysis as previously described.[7] Biological parentage was judged if more than four informative markers were compatible and other uninformative markers showed no discrepancies.

Expression Vectors

A full-length human *SPTAN1* cDNA was prepared by PCR with first-strand cDNA derived from a human lymphoblastoid cells (LCL) and an IMAGE clone (clone ID 5211391) as a template. The obtained *SPTAN1* cDNA was sequenced and confirmed to be identical to a RefSeq mRNA (amino acids 1–2477, GenBank accession number NM_001130438) except for two synonymous base substitutions that have been registered in dbSNP as rs2227864 and rs2227862. Site-directed mutagenesis via a KOD-Plus-Mutagenesis kit (Toyobo, Osaka, Japan) was used to generate *SPTAN1* mutants including c.6619_6621 del (p.E2207 del) and c.6923_6928 dup (p.R2308_M2309 dup). A C-terminal Flag-tag was introduced by PCR. All variant cDNAs were verified by sequencing. C-terminal Flag-tagged WT and mutant *SPTAN1* cDNAs were cloned into the pCIG vector[15,16] to express C-terminal Flag-tagged α-II spectrin as well as nuclear-localized EGFP. WT and mutant *SPTAN1* cDNAs were also cloned into the pCAG-EGFP-C1 vector, in which EGFP gene and multiple cloning sites of pEGFP-C1 vector (Clontech, Mountain View, CA) are introduced into a CAG-promoter vector,[15,16] to express N-terminal EGFP-tagged α-II spectrin.

For protein expression in *Escherichia coli*, WT and mutant *SPTAN1* cDNAs (amino acids 1445–2477, the last eight spectrin repeats and the EF hand domain) were cloned into pGEX6P-3 (GE Healthcare) to generate glutathione S-transferase (GST) fusion proteins. Human *SPTBN1* cDNAs (amino acids 1–1139, GenBank accession number NM_003128, including the actin binding domain and eight spectrin repeats) were prepared by PCR via first-strand cDNA derived from a human LCL, and were cloned into pET-24a (Merck, Darmstadt, Germany) to generate His-tag fusion proteins.

Protein Expression, Purification, and Binding Assay

Proteins were expressed in *Escherichia coli* BL21 (DE3). Bacteria were grown at 37°C in Lysogeny Broth media with 300 μg/ml ampicillin to a density yielding an absorbance at 600 nm of 0.8. Protein expression was then induced with 1 mM isopropyl-β-D-thiogalactoside (IPTG) at 20°C overnight. Cells were collected by centrifugation and lysed by sonication. Proteins were purified by

affinity chromatography with Glutathione Sepharose High Performance (GE Healthcare) for GST-α-II spectrin or HisTrap HP (GE Healthcare) for β-II spectrin-His. α-II spectrins were further purified by HiTrap Q HP (GE Healthcare) and Superdex-200 (GE Healthcare) columns in a buffer containing 150 mM NaCl, 20 mM sodium phosphate buffer (pH 7.5), and 2 mM dithiothreitol (DTT). β-II spectrin was further purified by Superdex-200 (GE Healthcare) columns in a buffer containing 1 M NaCl, 20 mM sodium phosphate buffer (pH 7.5), and 2 mM DTT.

For the GST pull-down assay to examine the assembly of α-II/β-II heterodimers, 0.5 μM GST-α-II spectrin (WT, del mut, or dup mut) or 1 μM GST were preincubated with 1 μM β-II spectrin-His for 1 hr at 4°C with gentle agitation in binding buffer containing 150 mM NaCl, 20 mM sodium phosphate buffer (pH 7.5), and 2 mM DTT. The reaction mixture (100 μl) was transferred onto an Ultrafree-MC (Millipore, Billerica, MA), containing 50 μl of a 75% slurry of Glutathione Sepharose 4B equilibrated in binding buffer, and incubated overnight at 4°C. Unbound proteins were recovered by centrifugation at 500 × g for 2 min. The beads were washed three times with the binding buffer. The bound molecules were eluted with a buffer containing 100 mM NaCl, 20 mM sodium phosphate buffer (pH 7.5), 5 mM DTT, 1 mM EDTA, and 50 mM reduced glutathione. The eluted fractions were analyzed by SDS-PAGE, and protein bands were visualized by staining with Coomassie brilliant blue. For the analytical gel filtration experiments, 3.3 μM GST-α-II spectrin (WT, del mut, or dup mut) were preincubated with or without 3.3 μM β-II spectrin-His for 3 hr at 4°C with gentle agitation in a binding buffer containing 150 mM NaCl, 20 mM sodium phosphate buffer (pH 7.5), and 2 mM DTT. The samples were analyzed by Superdex-200 column equilibrated in binding buffer. The eluted fractions were analyzed by SDS-PAGE and protein bands were visualized by staining with Coomassie brilliant blue.

Structural Prediction

The structure of human α-II spectrin was predicted by homology modeling with Phyre,[17] based on sequence homology between human α-II spectrin (1981–2315 aa) and chicken brain alpha spectrin (1662–1982 aa) (Protein data bank ID, 1U4Q).[18] The structure and positions of mutations were illustrated by PyMOL with the crystal structure of 1U4Q.

Circular Dichroism Measurements

For circular dichroism (CD) measurements, GST-α-II spectrin were digested with human rhinovirus 3C protease at 4°C, and then the GST-tag was removed by affinity chromatography with glutathione sepharose 4B (GE Healthcare). We measured far-UV CD spectra and estimated the secondary structure as previously described.[7] In brief, the experiments were performed in 20 mM sodium phosphate buffer (pH 7.5) containing 150 mM NaCl, 2 mM DTT with or without 1 mM $CaCl_2$, which stabilizes the structure of the EF hand domain. α-II and β-II spectrin concentration was adjusted to 1.7 μM (without $CaCl_2$) and 1.5 μM (with $CaCl_2$). Melting (transition midpoint) temperature (T_m) was calculated by fitting a sigmoid-function equation with KaleidaGraph (Synergy Software, Reading, PA). The data from three independent experiments were averaged and the SD was calculated. Similar results were obtained in the presence or absence of 1 mM $CaCl_2$.

Cell Culture, Transfection, and Immunofluorescence

For primary neuronal cultures for immunofluorescence, cortexes dissected from mice (embryonic days 14 to 15) were dissociated in 0.05% trypsin-EDTA solution (Invitrogen, Carlsbad, CA), and triturated with a Pasteur pipette. The dissociated cells were plated on 200 μg/ml poly-D-lysine (Millipore)/20 μg/ml laminin (Invitrogen)-coated glass coverslips at a density of 15,000 cells/cm^2. Expression vectors were introduced at the time of dissociation by electroporation, with the Amaxa Mouse Neuron Nucleofector kit (Lonza, Tokyo, Japan) according to the manufacturer's protocol (Program O-005), and 2 μg plasmid DNA per condition. After cortical neurons attached to coverslips, the medium was changed from normal medium (10% FBS in DMEM) to maintaining medium (2% B27 and 1 × penicillin-streptomycin-glutamine in Neurobasal [Invitrogen]). Half of the medium was replaced with an equal volume of maintaining medium every 4 days. LCLs were grown in RPMI 1640 medium supplemented with 10% FBS, 1 × antibiotic-antimycotic (Invitrogen), and 8 μg/ml tylosin (Sigma, Tokyo, Japan) at 37°C in a 5% CO_2 incubator. For the immunofluorescence imaging study, LCLs were plated on coated coverslips as described above for 3–6 hr.

Neurons and LCLs were fixed with 2% paraformaldehyde in PBS for 15 min and permeabilized with 0.1% Triton X-100 for 5 min. For detection of VGSCs, cells were fixed with methanol at −20°C for 10 min. Cells were then blocked with 10% normal goat serum for 30 min. Primary antibodies used for the study were shown in figure legends. Secondary antibodies, highly purified to minimize cross-reactivity, were used: Alexa-488-conjugated goat anti-mouse, anti-rabbit, and anti-chicken (Invitrogen), and Cy3-conjugated goat anti-mouse, anti-rabbit, and anti-chicken (Jackson ImmunoResearch, West Grove, PA). Coverslips were mounted with Vectashield (Vector Laboratories, Burlingame, CA) that contained 4,6-diamidino-2-phenylindole (DAPI) and visualized with an AxioCam MR CCD fitted to Axioplan2 fluorescence microscope (Carl Zeiss, Oberkochen, Germany). We captured images with Axio Vision 4.6 software (Carl Zeiss). Immunofluorescence of aggregated mutant α/β spectrins was much brighter than WT α/β spectrins, leading to constant short exposure time compared with the WT. For detection of ankyrinG and VGSCs, the exposure time was fixed in a series of experiments in order to enable direct comparison between different samples. For evaluation of ankyrinG and VGSC expression, 50 isolated transfected neurons were analyzed in each experiment, and representative cells were photographed. The results were confirmed at least in three independent experiments.

Electrophysiology

Mouse neocortices at embryonic day 15 were dissociated and plated on poly-L-lysine-coated plastic coverslips (Cell desk LF, MS-0113L; Sumitomo Bakelite, Tokyo, Japan) at a density of about 100,000 cells/cm^2. 1 μg of expression vector for either WT, del mut, or dup mut α-II spectrin was introduced at the time of dissociation by electroporation with an Amaxa Mouse Neuron Nucleofector kit (Lonza). Primary cortical neurons were cultured in neurobasal medium supplemented with B27 and penicillin-streptomycin-glutamine (Invitrogen). During the culture period, one-half of the medium was changed every day. Whole-cell patch-clamp recordings were obtained from mice neocortical neurons at 9 days in vitro (DIV) neuronal culture. A coverslip was assembled to recording chambers on the stages of upright microscopes (Olympus, Tokyo, Japan) and continuously perfused with oxygenated, standard artificial cerebrospinal fluid (ACSF) at a flow rate of 2 ml/min and a temperature of 30°C. The standard ACSF solution contained the following (mM): 126 NaCl, 2.5 KCl,

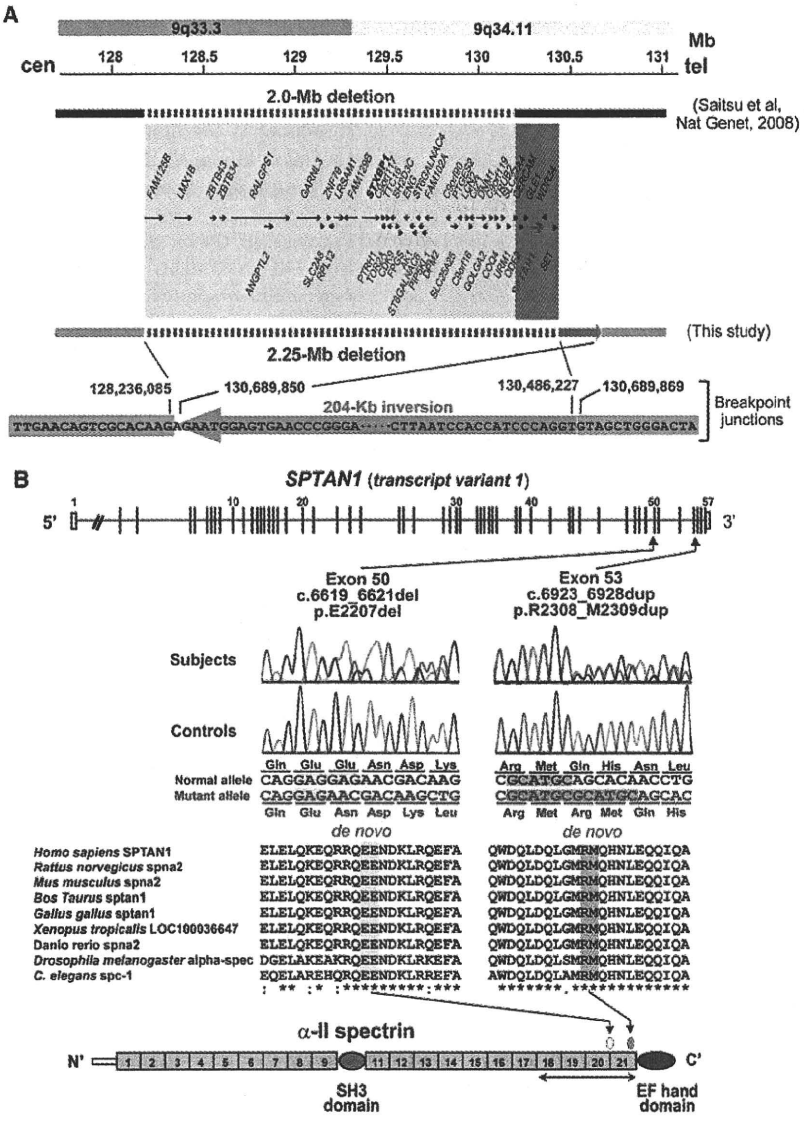

Figure 1. *SPTAN1* Aberrations in Individuals with West Syndrome and Cerebral Hypomyelination

(A) Genomic rearrangements at 9q33.3-q34.11 in subject 1. Top depicts chromosomal bands and genomic location (Mb) from the p telomere (cen, toward the centromere; tel, toward the telomere). Our previous study by BAC array could reveal the approximate size of the deletion (2.0 Mb) (horizontal line above boxes).[7] The deletion was newly analyzed by Affymetrix GeneChip 250K array and turned out to be 2.25 Mb in size (chr9:128,236,086-130,486,226) (UCSC genome browser coordinate [version Mar. 2006]) (horizontal line below boxes). Blue and red boxes indicate old and renewed deletion intervals, respectively. Five RefSeq genes (*ODF2*, *GLE1*, *SPTAN1*, *WDR34*, and *SET*) were newly found (in red box). The rearrangements include an unexpected 204 kb inversion (green arrow). Intact genomic regions are shown in sky blue.

(B) Schematic representation of *SPTAN1* (transcript variant 1) consisting of 57 exons (UTR and coding region are open and filled rectangles, respectively). Exon 37 of transcript variant 1 is missing in variant 2, the only difference between the two transcripts. Two distinct mutations were found at evolutionary conserved amino acids in triple helical repeats (spectrin repeats). All these mutations occured de novo. Homologous sequences were aligned with the CLUSTALW web site. α-II spectrin consists of 22 domains (numbered), including 20 spectrin repeats, an SH3 domain, and an EF hand domain. The mutations occurred within the last four spectrin repeats, which are required for α/β heterodimer association (bidirectional arrow).

1.25 NaH_2PO_4, 2.0 $MgSO_4$, 2.0 $CaCl_2$, 26.0 $NaHCO_3$, and 20.0 glucose. The images of cells were acquired with Olympus BX51 or BX61 microscopes equipped with electron-multiplying CCD (EMCCD) cameras, #C9100-13 or #C9100-02 (Hamamatsu Photonics, Hamamatsu, Japan), respectively. Transfected cells were selected for recordings by their fluorescence in the nucleus via a 40× water-immersion objective lens (UMPlanFI, Olympus). Membrane currents and membrane potentials were recorded with an Axopatch 700A and 200B amplifier, respectively. Signals were low-pass filtered at 10 kHz and digitized at 50 kHz by means of Digidata 1332A data-acquisition system (Molecular Devices, Tokyo, Japan). Passive membrane properties and action potentials were recorded with patch pipettes (5.8–8.0 MΩ) filled with the following intercellular solutions (in mM): 130 K-methanesulfonic acid, 10 KCl, 2 $MgCl_2$, 0.1 EGTA, and 10 HEPES (pH 7.3) with KOH. For current clamp experiments, cells were held at −60 mV by constant current injection as needed, and their firing pattern were recorded in response to sustained depolarizing current injections (500 ms duration, +10 pA increments) to analyze the input-output relationship in each cell. A single action potential was also evoked to determine their firing threshold. The injection current amplitude (10 ms duration) was increased in 2–10 pA increments from a subthreshold to an intensity well beyond threshold. Voltage-clamp studies for sodium currents were carried out with patch pipettes (5.8–8.0 MΩ) filled with the following intercellular solutions (mM): 145 tetraethylammonium-Cl, 15 NaCl, 2 $MgCl_2$, 10 EGTA, 10 HEPES, 3 MgATP, and 0.4 GTP (pH 7.4) with NaOH. Series resistance was usually below 20 MΩ and compensated by 70%–80%. The remaining linear capacitive and leakage currents were subtracted off-line by scaling average traces recorded at hyperpolarized voltages. Voltage-dependent inward sodium currents were elicited by 500 ms depolarizing steps in 5 mV increments from −90 to +10 mV at a holding membrane potential of −90 mV. For measuring the inactivation protocol of sodium currents, 500 ms long prepotentials started at − 90 mV and were incremented by 5 mV steps while the command potential was kept constant at −30 mV. The current elicited during each test pulse was normalized to the maximal current (I/Imax). Statistical

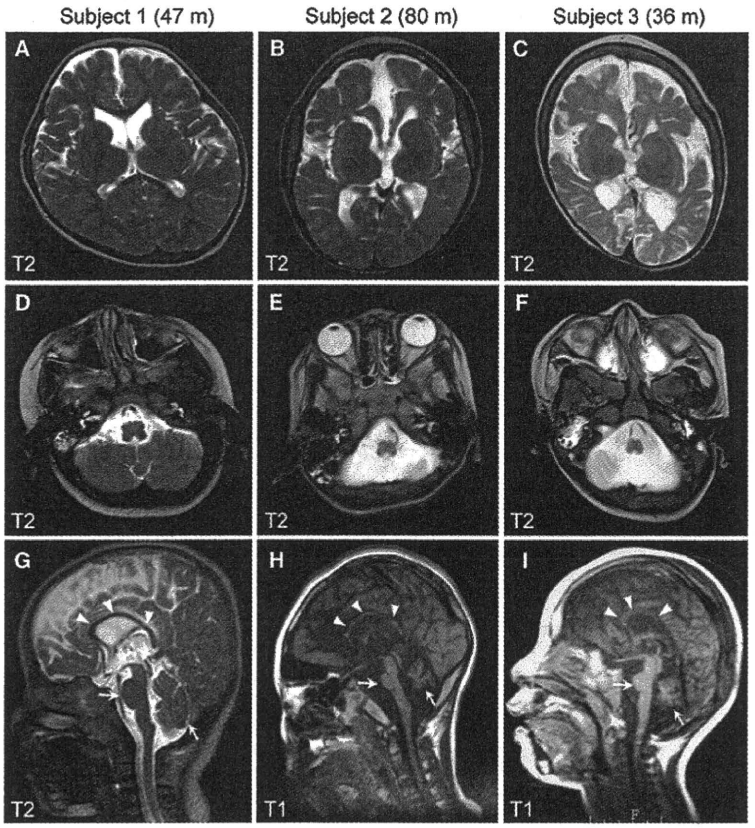

Figure 2. Brain MRI of Subjects with *SPTAN1* Aberrations at the Most Recent Developmental Stages

(A–C) T2-weighted axial images through the basal ganglia. Subject 1 (with a 2.25 Mb deletion) showed only slightly reduced white matter (A). By contrast, cortical atrophy and severe hypomyelination with strikingly reduced volume of white matter were evident, especially in the frontal lobes, in subjects with in-frame mutations (subjects 2 and 3) (B and C).

(D–I) T2-weighted axial images through the brainstem/cerebellum (D–F) and T2- (G) or T1-weighted midline sagittal images (H and I). Compared with subject 1 (D and G), subjects 2 (E and H) and 3 (F and I) show a thinned and shortened corpus callosum (arrowheads), severe atrophy of the brainstem, and hypoplasia and/or atrophy of the cerebellar hemispheres and vermis (arrows). m, months.

analyses were made with two-way repeated-measures ANOVA followed by a Bonferroni post-test for analysis of the input-output relationship and current amplitude at every voltage step. One-way ANOVA followed by Dunnet's posthoc test was applied for threshold, peak current, kinetics of action potentials, and passive membrane properties. The results are given as mean ± SEM, and threshold p value for statistical significance was 0.05. Statistical comparisons were performed with the Prism 4.0 (GraphPad software, La Jolla, CA).

Results

Identification of *SPTAN1* In-Frame Mutations

We previously reported a de novo 9q33.3-q34.11 microdeletion involving *STXBP1* in an individual with EIEE, who transited afterward to WS at the age of 3 months (subject 1).[7] Subject 1 was originally reported as one of four individuals (group A) who showed early onset WS and severe cerebral hypomyelination (as patient No. 2).[14] It is likely that haploinsufficiency of *STXBP1* caused EIEE and subsequent WS in subject 1;[7] however, no mutations of *STXBP1* were found in two of the remaining three individuals of group A (subjects 2 and 3, previously described as No. 1 and No. 3, and No. 4 was unavailable for this study).[14] Based on obvious severe hypomyelination of the group A individuals, we hypothesized that another gene within the deletion may contribute to the phenotype of group A, especially for severe hypomyelination. Re-examination of the deletion interval by genomic microarray and long PCR successfully determined the 2.25 Mb deletion and the associated 204 kb inversion (Figure 1A and see Figure S1). Among the 46 genes mapped within the deletion, *SPTAN1*, which encodes α-II spectrin, appeared to be a primary candidate because zebrafish α-II spectrin mutants showed impaired myelination.[13] We found de novo heterozygous mutations in *SPTAN1* in subjects 2 and 3 (parentage was confirmed in their respective families). Subject 2 has an in-frame 3-bp deletion (c.6619_6621 del) leading to p.E2207 del in the continuous helix region between the last two spectrin repeats, and subject 3 has an in-frame 6 bp duplication (c.6923_6928 dup, p.R2308_M2309 dup) within the last spectrin repeat (Figure 1B). These two mutations were absent in 250 Japanese normal controls (500 alleles). *SPTAN1* was further screened in six unrelated individuals with WS and hypomyelination similar to the phenotype of group A (not belonging to group B), but no mutations were found.

Phenotypes Associated with *SPTAN1* Aberrations

The clinical features of the three subjects with *SPTAN1* aberrations are summarized in Table S1. Subjects 2 and 3 showed severe spastic quadriplegia, no developmental progress, and poor visual attention. Epileptic seizures were resistant to various treatments. Subject 3 died of fulminant myocarditis at 3 years of age. In contrast, subject 1 showed slight psychomotor development with eye contact, but no head control. Her seizures have been well controlled. Brain MRI of subjects 2 and 3 revealed widespread brain atrophy including brainstem, hypoplasia, and/or atrophy of the cerebellar hemispheres and vermis, ventriculomegaly, a thinned and shortened corpus callosum, and severe hypomyelination with strikingly reduced white matter at 6 and 3 years of age, respectively (Figure 2). Of note, while subject 1 initially showed

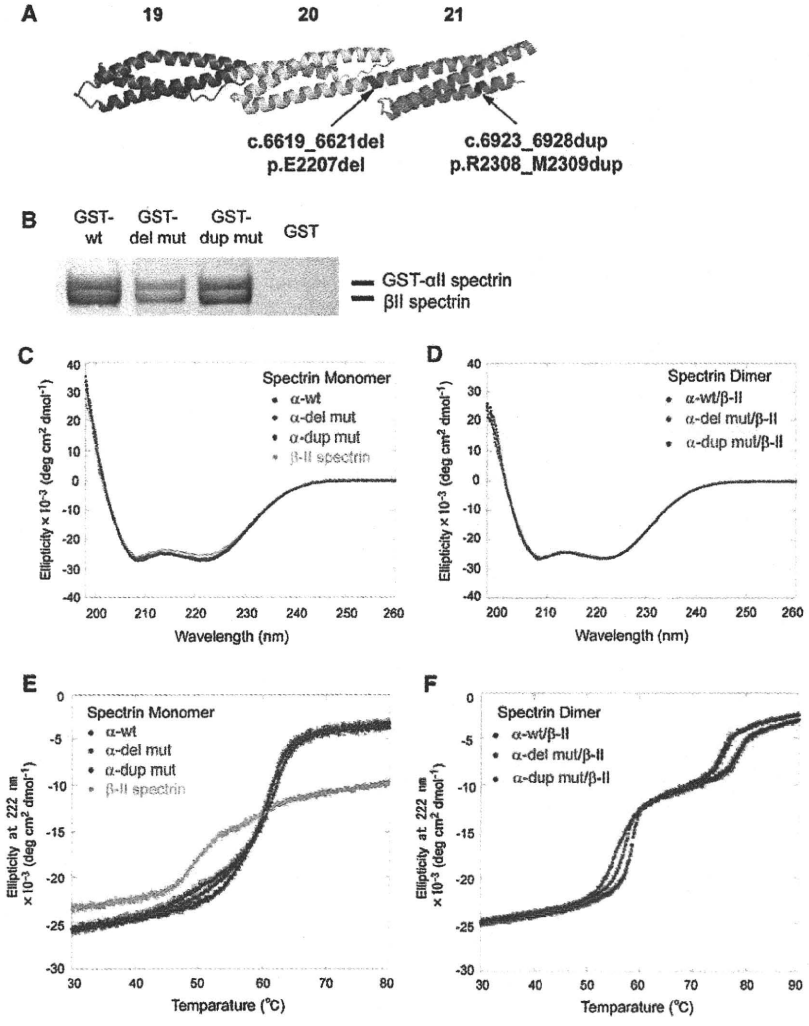

Figure 3. Mutational Effects on the α-II/β-II Spectrin Heterodimer

(A) Positions of the two mutations (c.6619_6621del, p.E2207 del in blue; c.6923_6928dup, p.R2308_M2309 dup in purple) in the predicted human α-II spectrin structure. Domains 19–21 (the last three spectrin repeats) are colored red, yellow, and green, respectively.

(B) GST pull-down assay of a recombinant GST-tagged α-II spectrin/β-II spectrin heterodimer. The WT and two mutant α-II spectrins could form heterodimers with β-II spectrin at comparable levels. β-II spectrin did not show any binding to GST alone.

(C–F) CD spectra (C and D) and CD melting curves (E and F) at 222 nm of the WT, del mut, and dup mut of α-II spectrins and β-II spectrin as a monomer (C and E) and as heterodimers of the WT, del mut, and dup mut of α-II spectrins with β-II spectrin (D and F). CD spectra showed no difference in the helical content of the WT and mutant α-II spectrin monomers and heterodimers with β-II spectrin (C and D). The WT and mutant α-II spectrin monomers are unfolded at 60°C, whereas β-II spectrin is unfolded around at 50°C (E). In contrast, dimers of WT and mutant α-II spectrins with β-II spectrin are partly dissociated and accompanied with denaturation of a local part of the monomers at 50°C–60°C (*Tm* [°C]: 58.362 ± 0.059 [WT], 55.617 ± 0.047 [del mut], 57.110 ± 0.077 [dup mut]) and completely unfolded at 70°C–80°C (*Tm* [°C]: 78.515 ± 0.327 [WT], 75.813 ± 0.115 [del mut], 75.267 ± 0.469 [dup mut]) (F). The thermostability of the heterodimers is obviously different between the WT and the mutants. Each dot represents the average of three repeated experiments; error bars, SD.

striking hypomyelination of cerebral cortex and thin corpus callosum at 12 months of age,[14] she completed myelination and showed only slightly reduced white matter at 4 years of age (Figure 2). The apparent differences of drug intractability and severity of cerebral hypomyelination and brainstem/cerebellum atrophy (subjects 2 and 3 versus subject 1) strongly suggested dominant-negative, rather than loss-of-function, effects of the in-frame mutations.

Characterization of α-II/β-II and α-II/β-III Heterodimers

The mutations were predicted to affect formation of α/β spectrin heterodimers, because they were located at the initial nucleation site of the α/β spectrin heterodimer[19] (Figures 1B and 3A). To examine the properties of the α-II spectrin mutants in the context of dimer formation, we purified recombinant WT and the two mutant α-II spectrin proteins (c.6619_6621 del, p.E2207 del and c.6923_6928 dup, p.R2308_M2309 dup, designated as del mut and dup mut, respectively). Both GST pull down and analytical gel filtration experiments revealed that the two mutants could form heterodimers with β-II spectrin at comparable levels to the WT (Figure 3B). Circular dichroism (CD) spectra indicated no difference of helical content between WT and mutant α-II spectrin monomers, nor between WT and mutant α-II/β-II heterodimers (Figures 3C and 3D). However, CD melting experiments revealed that the mutations apparently affected the thermostability of α-II/β-II heterodimers (Figure 3F). Considering the melting curves of α-II and β-II spectrin monomers (Figure 3E), the melting transitions of heterodimers in the ranges of 50°C–60°C and 70°C–80°C represent partial dissociation of heterodimers to monomers accompanied by denaturation of a local part of the monomers and complete denaturation, respectively (Figure 3F). Apparent differences of melting curves in the 50°C–60°C and 70°C–80°C ranges suggested that the mutations alter the stability of α-II/β-II heterodimers.

The effect of the mutations was further clarified by transient expression in cultured mouse cortical neurons. α-II

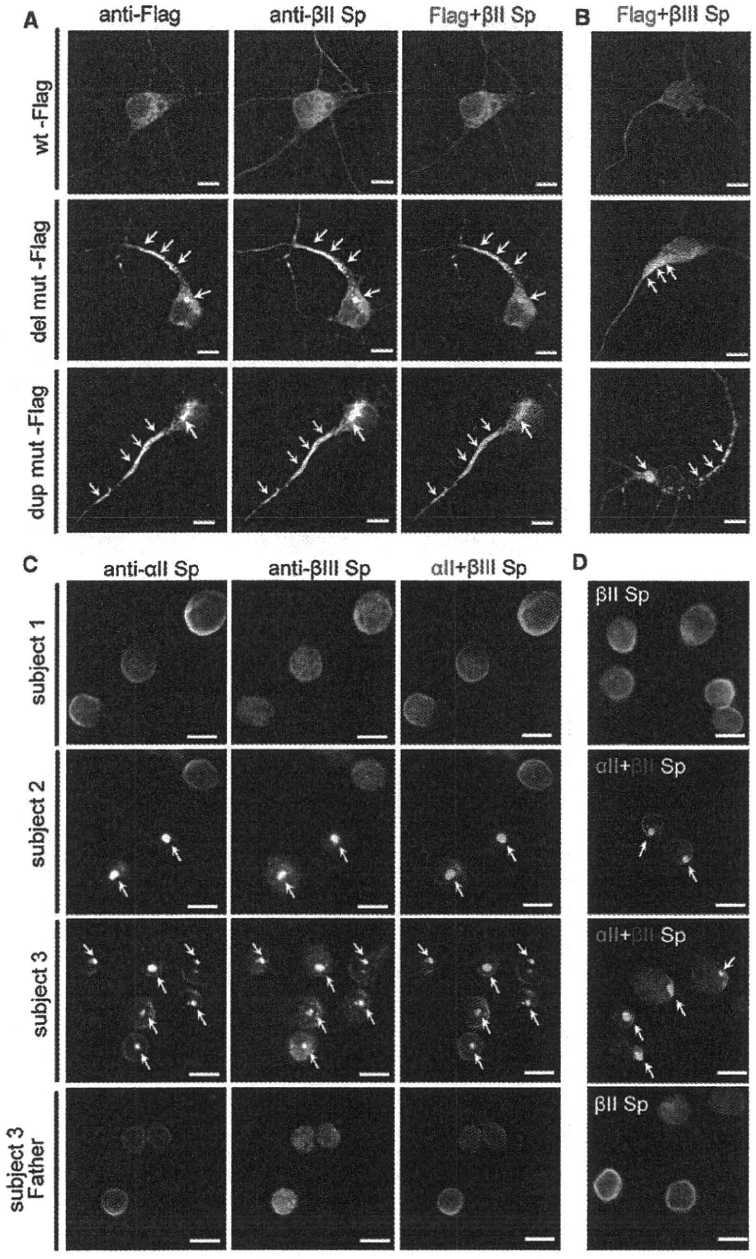

Figure 4. Mutant α-II Spectrin Causes Aggregation of α/β Spectrin Heterodimer

(A and B) Expression of the WT and the two mutant α-II spectrins at 7 DIV. Flag tagged-α-II spectrin (WT-Flag) showed similar expression to endogenous α-II spectrin (top, compare with Figure S2A). However, two mutant α-II spectrins (del mut-Flag and dup mut-Flag) showed aggregation predominantly in cell bodies and axons (arrows), and these aggregations were colocalized with β-II and β-III spectrins (middle and bottom). (C and D) Aggregation of endogenous α/β spectrin heterodimers were found in LCLs derived from two subjects harboring *SPTAN1* in-frame mutations. In LCLs of subject 2 (with c.6619_6621del, p.E2207del) and subject 3 (with c.6923_6928dup, p.R2308_M2309dup), aggregation of α-II/β-III (C) and α-II/β-II (D) spectrin heterodimers were frequently observed (middle two panels, arrows), while such aggregation was never observed in subject 1 (top). LCL of subject 3's father did not show any such aggregation (bottom).

The scale bars represent 10 μm. The following primary antibodies were used: mouse anti-α-II spectrin (1:400 dilution; clone D8B7; Abcam, Tokyo, Japan), mouse anti-β-II spectrin (1:600 dilution; clone 42/B-spectrin II; BD Transduction laboratories, San Jose, CA), rabbit anti-β-II spectrin (1:100 dilution; Abcam), rabbit anti-β-III spectrin (1:400 dilution; Abcam), mouse anti-Flag M2 (1:1000 dilution; Sigma), and rabbit anti-DDDDK-Tag (1:2000 dilution; MBL, Nagoya, Japan).

spectrin has been shown to be expressed in mouse brain, especially in neuronal axons.[20] In cultured cortical neurons, α-II spectrin was expressed at cell extensions and the periphery,[21] overlapping with the expression of β-II and β-III spectrins (Figure S2). We generated two α-II spectrin expression vectors: one was a dual expression vector of C-terminally Flag-tagged α-II spectrin and nuclear EGFP (Flag-nucEGFP), and the other was an N-terminally EGFP-tagged (EGFP) α-II spectrin. Tagged WT α-II spectrin from both vectors showed similar expression to endogenous α-II spectrin (Figure 4A and Figure S2). Notably, the two mutant α-II spectrins (del mut and dup mut) showed aggregation, predominantly in cell bodies and axons (Figure 4A, arrows, and Figure S2). Double immunostaining revealed that these aggregations were colocalized with β-II and β-III spectrins (Figures 4A and 4B, arrows, and Figure S2), indicating that unstable α-II/β-II and α-II/β-III spectrin heterodimers were involved in the aggregation. Remarkably, LCLs established from subjects 2 and 3 also showed similar aggregation, while LCLs of subject 1 and subject 3's parents showed no aggregation (Figures 4C and 4D, arrows). These findings indicated dominant-negative effects of the mutations for the integrity of α-II/β-II and α-II/β-III spectrin heterodimers. Immunostaining against β-IV spectrin did not show its involvement in the mutant aggregation (Figure S2).

Effects of the *SPTAN1* Mutations on ankyrinG and VGSC Clustering at AIS

Spectrins play important roles in clustering specific integral membrane proteins at high density in specialized regions of the plasma membrane.[8] To examine the effects of α/β spectrin heterodimer impairment, protein localization at AIS was examined, where ankyrinG and VGSC are clustered and action potentials are initiated.[22,23] At 9

DIV, expression of ankyrinG and VGSC were clustered at AIS when WT Flag-nucEGFP was transfected (Figures 5A and 5B, top). In contrast, clustering of ankyrinG and VGSC was disturbed in the presence of extensive α-II (mut)/β-II and α-II (mut)/β-III spectrin aggregation (Figures 5A and 5B, middle and bottom). Interestingly, whole-cell current clamp recordings from cortical neurons expressing mutant α-II spectrins showed impairment of repetitive action potential elicitation and elevated threshold of action potential compared with those expressing the WT (Figure 6A), while there were no significant differences in the passive membrane properties among the genotypes (Table S3). Recordings of whole-cell sodium currents with conventional activation and inactivation protocols revealed that expression of the mutants caused a significant depolarizing shift in activation compared with the WT, indicating increased threshold of sodium currents (Figures 6B and 6C). These mutants did not affect any of the activation kinetic properties (10%–90% rise time) (Figure 6E), the voltage dependence of inactivation (Figures 6F and 6G), or the whole cell capacitance (Table S3). However, peak sodium current densities were substantially reduced in cells expressing dup mut or del mut (Figure 6D). Divergent distribution of VGSC at AIS can increase the action potential threshold probably resulting from the waste of charging current across the axonal membrane;[24] therefore, the abnormal spike initiation observed in two mutants could be caused by the disturbance of VGSC clustering at AIS.

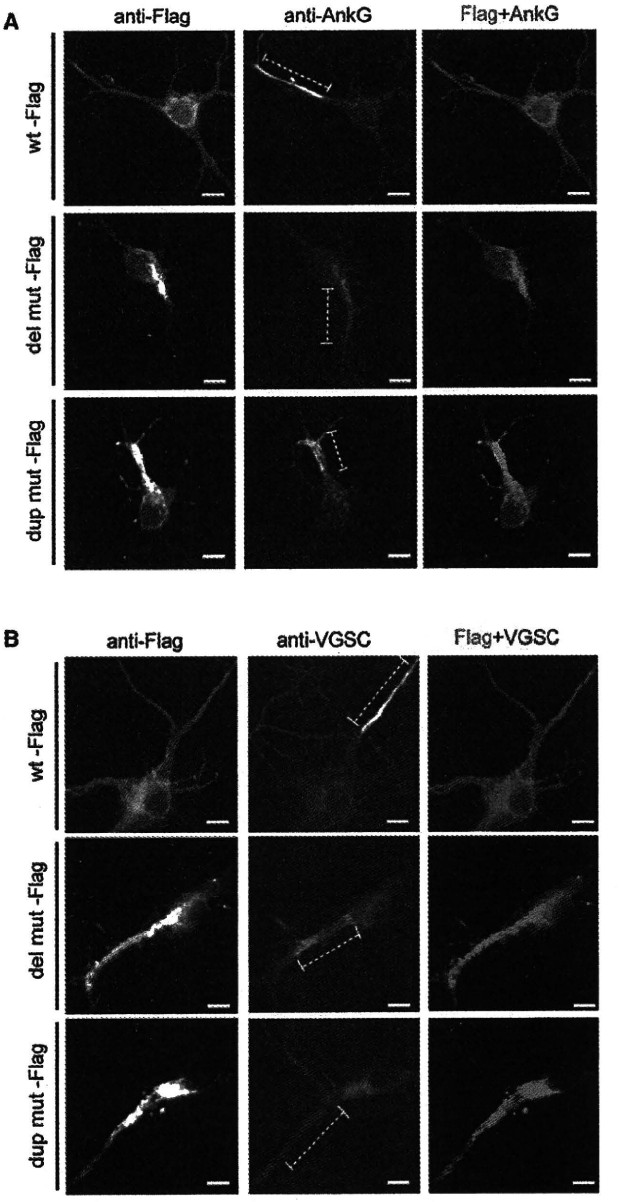

Figure 5. Transient Expression of Mutant α-II Spectrin Led to Disturbance of AnkyrinG and VGSC Clustering at AIS
Expression of ankyrinG (AnkG) (A) and VGSC (B) at 9 DIV. When WT α-II spectrin is expressed, neurons showed clustering of AnkG and VGSC at AIS (top). However, clustering of AnkG and VGSC were disturbed in the presence of extensive α/β spectrin aggregation when mutant α-II spectrins (both the del mut and the dup mut) were expressed (middle and bottom). AIS regions are shown by dashed lines. The scale bars represent 10 μm. The following primary antibodies were used: mouse anti-ankyrinG (1:100 dilution; clone 4G3F8; Santa Cruz Biotechnology, Santa Cruz, CA), mouse anti-pan sodium channel (for VGSC) (1:100 dilution; clone K58/35; Sigma), and rabbit anti-DDDDK-Tag (1:2000 dilution; MBL).

Discussion

We have shown that two de novo in-frame mutations of *SPTAN1* cause early-onset WS with spastic quadriplegia, poor visual attention, and severe developmental delay. Brain MRI of the two subjects showed severe cerebral hypomyelination, decreased white matter, widespread brain atrophy including brainstem, hypoplasia and/or atrophy of the cerebellum, and a thinned and shortened corpus callosum. On the other hand, mutations of *STXBP1* cause EIEE, and brain MRI of individuals with *STXBP1* mutations showed no structural malformations in contrast with striking structural abnormalities with *SPTAN1* mutations.[7] Among three subjects harboring *SPTAN1* aberrations, subject 1 deleted both *SPTAN1* and *STXBP1* heterozygously.[7] Similar to individuals with *STXBP1* mutations, subject 1 had distinctive features of EIEE, such as early onset of spasms, suppression-burst pattern on electroencephalogram, transition to West syndrome, and severe developmental delay.[7] Therefore it is likely that haploinsufficiency of *STXBP1* caused EIEE and subsequent WS in subject 1. However, subject 1 additionally showed apparent hypomyelination of cerebral cortex and thin corpus callosum at 12 months of age,[14] which appeared to be distinct from clinical features caused by *STXBP1* mutations. Based on these differences, we hypothesized that another gene within the deletion may contribute to severe hypomyelination, and successfully found two de novo in-frame mutations of *SPTAN1* in subject 2 and 3 of